Sensors and Controls for Automated Manufacturing and Robotics

Edited by

K. A. STELSON

L. M. SWEET

Sensors and Controls for Automated Manufacturing and Robotics

presented at

THE WINTER ANNUAL MEETING OF
THE AMERICAN SOCIETY OF MECHANICAL ENGINEERS
NEW ORLEANS, LOUISIANA
DECEMBER 9-14, 1984

sponsored by

THE DYNAMIC SYSTEMS AND CONTROL DIVISION, ASME

edited by

K. A. STELSON
UNIVERSITY OF MINNESOTA

L. M. SWEET
GENERAL ELECTRIC COMPANY

THE AMERICAN SOCIETY OF MECHANICAL ENGINEERS
United Engineering Center 345 East 47th Street New York, N.Y. 10017

Library of Congress Catalog Card Number 84-72454

Statement from By-Laws: The Society shall not be responsible for statements or opinions advanced in papers . . . or printed in its publications (B7.1.3)

Any paper from this volume may be reproduced without written permission as long as the authors and publisher are acknowledged.

Copyright © 1984 by
THE AMERICAN SOCIETY OF MECHANICAL ENGINEERS
All Rights Reserved
Printed in U.S.A.

FOREWORD

This volume is a collection of papers that address some of the crucial issues of automated manufacturing, particularly issues of flexible automation. A quick scan of the Table of Contents will reveal that the papers are not very closely related so far as academic discipline is concerned. Topics ranging from metal deformation to computer vision are represented in a volume that ostensibly deals with sensors and controls. The complexity of a flexibly automated factory necessitates an interdisciplinary approach, and at the very least, it is hoped that workers in one area appreciate the importance of other areas in advancing automated manufacturing technology.

The interdisciplinary nature of the problem of flexible automation notwithstanding, control theory has a central role to play in both organizing the automated factory as a whole, and in controlling unit processes. The ability of machines in the automated factory to react intelligently in an uncertain environment is highly desirable if not necessary. Improved feedback controls and sensors are needed to achieve this objective. Also, the crucial role of modelling cannot be overemphasized. In many cases, the inadequacy of models of robot response, metal cutting metal forming and solidification processes has inhibited automation. Lastly, the combination of papers on manufacturing and robotics in a single volume is a natural one, because robots are an essential component of any flexible automated factory.

The editors would like to thank the efforts of all those who made this volume possible. We would like to congratulate the authors, who have produced high quality papers on a very tight schedule. The careful comments of the reviewers have also contributed much to the quality of the papers. The efforts of A. Galip Ulsoy of the University of Michigan, David E. Hardt of Massachusetts Institute of Technology, and W. J. Book of Georgia Institute of Technology are highly appreciated. They have organized the sessions on metal cutting, welding and solidification processes, and robotics, respectively.

Kim A. Stelson

Larry M. Sweet

CONTENTS

试读结束：需要全本请在线购买： www.ertongbook.com

IDENTIFICATION OF DISCRETE TIME DYNAMIC MODELS FOR MACHINE TOOL FEED DRIVES

P. K. Kulkarni, Graduate Student and **K. Srinivasan**, Associate Professor
Department of Mechanical Engineering
The Ohio State University
Columbus, Ohio

ABSTRACT

An empirical technique for determining accurate linear discrete time models of machine tool feed drive dynamics is described here. The equation error is minimized in a least squares sense by appropriate selection of constant coefficients in a difference equation relating sampled values of the input and output variables. The identification method is evaluated based on an accurate digital computer simulation of a typical machine tool feed drive. The appropriate model order is determined by successful application of available tests for model order selection in parameter estimation problems. Two types of models are developed: pulse transfer function models and time series models. The models obtained represent feed drive behaviour more accurately than do other models reported in current literature. The identification technique is mechanizable. When used in conjunction with mechanizable controller design procedures, the identification technique described here should lead to the development of digitally controlled high performance feed drive servomechanisms.

NOMENCLATURE

$\tilde{A}$	Integral measure of step response
$\underline{A}(n)$	Matrix of measurements
$a_1,\ldots,a_m$	Model parameters
$b_0,\ldots,b_m$	Model parameters
$\underline{C}(n)$	Matrix of output samples
$C(z), C_m(z)$	Z-transform of $c(k)$ and $c_m(k)$
C_1, C_2	Viscous damping coefficients for drive train and tool slide
$c(k)$	Output sequence

$\hat{c}(k)$	Estimate of c(k)
$c_m(k)$	Model output sequence
D(s)	Model matrix determinant
DE	Determinant of $\underline{M}$
DV	Determinant ratio
E_r	Average of the squared response error
$e_e(k)$	Equation error sequence
F_L	Cutting tool load on slide
G(z)	Pulse transfer function
$G_{cv}(s)$	Velocity loop cascade compensator transfer function
$G_d(s)$	Motor shaft velocity to cutting load transfer function
$G_m(s)$	Open velocity loop feed drive transfer function
$G_r(s)$	Mechanical transmission transfer function
J	Sum of squares of equation error
K	Axial spring constant of ball screw
K_b	Motor back emf constant
K_c	Position loop controller gain
K_e	Encoder position feedback gain
K_g	Model steady state gain
K_{SCR}	SCR amplifier average gain
K_t	Motor torque constant
K_{tac}	Velocity feedback transducer gain
K_v	Velocity loop controller gain
L_a	Armature circuit inductance
$\underline{M}$	Information matrix
M_1	Equivalent mass of motor and ball screw inertias
M_2	Mass of nut and slide assembly
m	model order
m_{ij}	Element of $\underline{M}$
N_c	Condition number
$\underline{P}$	Covariance matrix
$\underline{R}(n)$	Matrix of input samples

$R(z)$	Z-transform of $r(k)$
R_a	Armature resistance
$r(k)$	Input sequence
s	Laplace operator
T	Discretization interval
t	Continuous time
u_0	Step input magnitude for $r(k)$
V_a	SCR control signal
V_m	Motor armature voltage
V_{rv}	Motor velocity reference signal
$\underline{x}$	Estimate of parameter vector
$x_p, \dot{x}_p$	Slide position and velocity
x_r	Slide position reference signal
z	Z transform operator
α	Rotation to linear motion conversion factor
$\theta_m, \dot{\theta}_m$	Motor angular position and velocity
$\underline{\phi}(k)$	Vector of measurements
$\tau_1, \tau_2, \tau_3, \tau_4$	Velocity loop compensator time constants

INTRODUCTION

High performance requirements on machine tool feed drives can be satisfied by the use of complex control algorithms and/or by mechanical design improvements. Digital controllers are particularly attractive for such applications since they provide for enhanced reliability, better diagnostic techniques and greater flexibility [1]. Lower hardware costs resulting from advances in microelectronics have also made digital controllers very popular in recent years. However, in practice, it has been difficult to realize the full potential of digital controllers for improving feed drive performance.

Accurate dynamic models of feed drives are essential for the design of complex digital control algorithms. However, reported work in the literature on digital feed drive control has, with a few exceptions, used only simple linear first or second order models of feed drive dynamic behaviour [2,3]. The importance of modeling structural resonances for the control of high performance feed drives has been noted by Douglass et al [4] and by Stute et al [5]. In view of the presence of pronounced nonlinearities in machine tool feed drives, such as Coulomb friction and the relationships governing SCR firing, experimental techniques for identifying discrete time models of feed drive dynamics are very useful and have been described by Bollinger et al [1] and Van Brussel and Vastmans [6]. The technique described in these references are, however, not versatile enough to model structural resonances. Previous modeling work has also ignored feed drive response to cutting forces in spite of its practical significance. The usefulness of modeling this effect is that it would enable feed drive stiffness to be improved by cutting force measurement and appropriate controller design, in applications where this is desirable.

Two identification techniques to obtain more accurate models of feed drive dynamic behaviour have been described and evaluated by Kulkarni et al [7]. Firstly, discrete time models were generated by deriving continuous time models based on analytical and/or empirical methods and then forming discrete time versions of these models. Secondly, existing identification techniques for direct determination of discrete time models with reduced computational requirements and hence suitable for microprocessor implementation [8] were modified and evaluated. Neither of the identification techniques was easily mechanizable. Model accuracy was good but could be improved further by direct determination of the 2n-1 coefficients in an n^{th} order pulse transfer function so as to explicitly minimize a measure of the modeling error. Such a technique would be mechanizable, which is advantageous if the controller design and/or adjustment is also automatically performed. In fact, the lack of mechanizable identification and controller design procedures for more sophisticated control algorithms is one of the reasons for the continuing popularity of simpler but well tested analog or digital feed drive control algorithms, even in current generation CNC machine tools.

An empirical technique for determining accurate linear discrete time models of machine tool feed drive dynamics is described here. The feed drive models include the effects of command inputs to the feed drive and of cutting forces. The equation error is used as a measure of modeling error and is minimized in a least squares sense by appropriate selection of constant coefficients in a difference equation relating sampled values of the input and output variables. The identification method is mechanizable and is evaluated based on an accurate digital computer simulation of a typical machine tool feed drive. The appropriate model order is determined by application of available tests for model order selection in parameter estimation problems. The models obtained here are evaluated for a variety of feed drive operating conditions of interest and significance and compared with models described in an earlier paper [7]. The implications of the proposed models for controller design are summarized.

Feed Drive Dynamic Model and Simulation Details

The Advanced Continuous Simulation Language (ACSL) [9] was used to implement a dynamic model of the feed drive. The model parameters chosen correspond to a 3-axis contouring horizontal machining center. The model proposed by Middleditch [10] for the mechanical components of the feed drive was incorporated in the simulation. The model includes the lowest resonant frequency of the feed drive transmission and nonlinear Coulomb friction as well. The SCR power amplifier is of the single phase, full wave type and drives a permanent magnet DC servomotor coupled directly to a lead screw. Details of the digital computer simulation, particularly the nonlinear SCR amplifier operation, are given by Johnson [11].

A block diagram of the linearized feed drive model for a single axis is shown in Figure 1. The symbols are defined in the Nomenclature section of the paper. The SCR amplifier nonlinearity is omitted in the block diagram and it is represented by a constant gain term, K_{SCR}, though the simulation includes an accurate representation. Analog control of the velocity loop is implemented by using the motor shaft velocity as the feedback variable. The compensator in the forward path of the velocity loop includes lag compensation at low frequencies to improve the feed drive stiffness to cutting loads. Lead compensation is implemented at high frequencies to increase the closed velocity loop bandwidth without significantly increasing the excitation of the mechanical resonance.

Details of the Identification Method

The feed drive dynamic model to be obtained will be used in conjunction with mechanizable controller design procedures. Off-line identification and controller parameter selection are quite adequate for the application since the feed drive parameters are subject only to long term change due to factors such as component degradation and wear. Moreover, since controller design is generally more conveniently performed with parametric models, the result of the identification method should be a parametric model such as a pulse transfer function.

A linear model of the feed drive dynamics is preferred because of the resulting simplification of the identification [12] and controller design problems. The SCR amplifier is a highly nonlinear element and would result in the feed drive behaviour being nonlinear. However, the closed motor shaft velocity loop behaviour is less strongly nonlinear because of the linearizing effect of feedback [7]. Though a linear model of the overall feed drive dynamics is acceptable for this reason, proper evaluation of any proposed model should include evaluation of model accuracy for a variety of input types and sizes. The controller design procedure should also emphasize robustness of the controller.

A deterministic formulation of the identification method is used because of the relative insignificance of random effects on the system dynamic behaviour. Sampled values of the input and output signals, generated by periodic sampling of the signals, are used to determine the coefficients in a pulse transfer function. Figure 1 indicates the need for determining models of the feed drive response to the reference input V_{rv} to the closed velocity loop and cutting loads F_L. Though the identification method described below can be modified easily to accommodate the multiple-input case, application of the test inputs one at a time is more practical. Hence the identification method is formulated below for the single-input, single-output case.

Let the input and output sequences be r(k) and c(k) and their one-sided Z-transforms R(z) and C(z) respectively.

$$R(z) = \sum_{k=0}^{\infty} r(k) z^{-k}$$

$$C(z) = \sum_{k=0}^{\infty} c(k) z^{-k} \qquad (1)$$

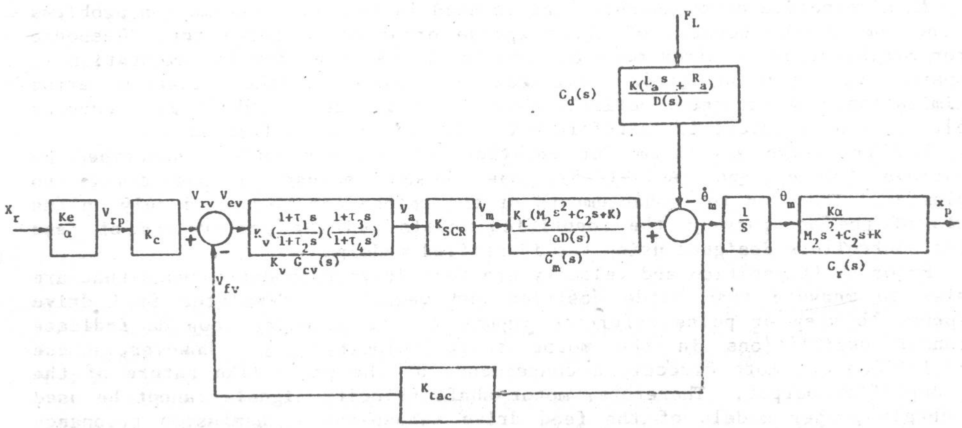

$$\begin{aligned} D(s) = {} & (M_1 M_2 L_a \alpha)s^4 + (M_1 M_2 \alpha R_a + M_2 C_1 L_a \alpha + M_1 C_2 L_a \alpha)s^3 \\ & + (M_1 C_2 R_a + M_2 C_1 R_a \alpha + M_1 K L_a \alpha + M_2 K L_a \alpha + C_1 C_2 L_a \alpha)s^2 \\ & + (M_1 R_a K\alpha + M_2 R_a K\alpha + C_1 K L_a \alpha + C_2 K L_a \alpha + C_1 C_2 R_a \alpha + C_2 \frac{K_b K_t}{\alpha})s \\ & + (C_1 R_a K\alpha + C_2 R_a K\alpha + \frac{K_b K_t K}{\alpha}) \end{aligned}$$

Figure 1. Block Diagram of Linearized Feed Drive Model for a Single Axis

试读结束：需要全本请在线购买： www.ertongbook.com

The identification method determines parameters in the pulse transfer function G(z) that best represents the ratio C(z)/R(z) of the transforms C(z) and R(z).

$$G(z) = \frac{b_0 + b_1 z^{-1} + \ldots + b_m z^{-m}}{1 + a_1 z^{-1} + \ldots + a_m z^{-m}} = \frac{C(z)}{R(z)} \quad (2)$$

The error measure considered here is the equation error $e_e(k)$ defined as

$$e_e(k) = c(k) - \left\{ \sum_{i=0}^{m} b_i r(k-i) - \sum_{i=1}^{m} a_i c(k-i) \right\}$$

$$= c(k) - \hat{c}(k) \qquad k = 0,1,\ldots,n \quad (3)$$

where $\hat{c}(k)$ is equal to the expression within curly brackets and is the predicted output for the k^{th} instant based on the measured input and output sequences. The sum of the squares of the equation error sequence over the period of observation, J, is minimized by appropriate selection of the parameters $b_0,\ldots,b_m$ and $a_1,\ldots,a_m$ in equation (3).

$$J = \sum_{k=0}^{n} e_e^2(k) \quad (4)$$

The problem, as formulated, is a standard parameter estimation problem. A recursive algorithm for the parameter estimation is summarized in Appendix A. Details of the derivation can be found in standard textbooks on parameter estimation [13].

The equation error minimization scheme described above provides accurate parameter estimates if the system being identified is linear and if the signal to noise ratio is high. In the presence of measurement noise, parameter estimates are biased. Enhancements of the simple least squares method to reduce the bias have been devised primarily for the case of random measurement noise [14]. Their usefulness in the present application, where system nonlinearity is more significant than measurement noise, has yet to be established.

An alternative error measure that is used in parameter estimation problems is the sum of the squares of the response error or output error. Response error minimization requires more computational resources for implementation as compared to equation error minimization. Also, unlike equation error minimization, the parameter estimation scheme is iterative and may not converge [15]. Such a technique is therefore not amenable to mechanization.

The recursive algorithm for equation error minimization, described by equations (1)-(4) and (A-1)-(A-5), was chosen because it was simple to implement. The need for enhancements of the method can be judged only on the basis of the accuracy of the identified models and the performance of feed drive controllers designed using the identified models.

Motor shaft position and velocity are feed drive response signals that are easier to measure than slide position and velocity. Simulated feed drive response to step or pulse reference inputs to the velocity loop do indicate resonant oscillations in the motor shaft velocity [7]. However, these oscillations are more directly a consequence of the pulse-like nature of the SCR amplifier output. Therefore, motor shaft velocity signals cannot be used to obtain proper models of the feed drive mechanical transmission resonance unless the sampling action of the SCR amplifier is explicitly modeled. The resulting discrete-time feed drive model would involve multirate sampling and would be too complex to be useful.

Slide position and velocity measurements provide more information on the transmission resonance than motor shaft position and velocity and are chosen as the feed drive response signals here. The result is a better numerical conditioning of the matrices $(\underline{A}^T(n)\underline{A}(n))$ to be inverted, as required by equation (A-3).

Step and pulse reference inputs to the closed velocity loop are expected to be adequate to excite the mechanical transmission resonance, especially if slide velocity or position are measured. A step input of the disturbing force F_L is appropriate for modeling feed drive compliance to cutting loads since the compliance has dominant low frequency components. All of the test inputs are easy to implement in practice.

A small value of the sampling interval improves the accuracy of the discrete time model of the feed drive, since such a model really represents the discrete equivalent of a continuous time system subject to continuously varying input signals. Since the model is to be used for digital controller design, the sampling interval depends also on the required closed feed drive position loop bandwidth and the control law computation time. A sampling interval of 4 msec seems appropriate here for modeling accuracy and control effectiveness. This time interval is also adequate for reasonably complex control computations to be performed by a control computer based on an Intel 8086/8087 processor - coprocessor system [16].

A lower limit on the model order m in equation (2) is determined by the maximum time delay in the SCR amplifier operation and the sampling interval chosen. For the single-phase, full-wave SCR amplifier and a 60 Hz power line frequency, the maximum time delay is 8.33 msec. The minimum model order m, for a sampling interval of 4 msec, is three. The minimum model order would be lower for a three-phase SCR amplifier.

Unbehauen and Göhring [17] have described a number of tests for the determination of the correct model order in parameter estimation problems. The testing methods, when performed together, were shown to determine the correct model order accurately. Five of these tests are relevant for the current application and are described briefly in Appendix B, along with another test suggested by Isermann [18]. The different model order tests were generally consistent in their indication of the appropriate model order, as described in the results below.

Identification Results

Determination of $\dot{x}_p(z)/V_{rv}(z)$

The response of the slide velocity $\dot{x}_p$ to a step input of the reference signal V_{rv} to the closed velocity loop ($F_L = 0$) was used to determine the pulse transfer function $\dot{x}_p(z)/V_{rv}(z)$. The magnitude of the step input was 1.0 Volt and corresponded to a slide velocity of 2.65 m/min (105 in/min). This value of slide velocity is about 25% of the maximum slide traverse velocity of 10.00 m/min (400 in/min). 100 samples each of the input and output signals were obtained at a sampling rate of 250 Hz and used by the identification algorithm. The slide velocity was used as the output signal instead of the slide position since the signal oscillations due to the transmission resonance were more pronounced in the former.

Pulse transfer function models of the form of equation (2) and of orders two to six were identified for $\dot{x}_p(z)/V_{rv}(z)$. Table 1 indicates the results of applying the model order tests described in Appendix B. The error values listed are the average values of the squared errors per sampling instant. The equation error is the error measure minimized by the identification algorithm and is about an order of magnitude lower than the response error. It is the magnitude of the response error that is indicative of model accuracy. Though direct minimization of the response error is difficult as mentioned above, the results indicate that reducing the equation error does reduce the response error.

Model Order, m	2	3	4	5	6
Equation error cm^2/sec^2 (ft^2/sec^2)	0.2483 (0.2673×10^{-3})	0.3449×10^{-2} (0.3172×10^{-5})	0.3014×10^{-2} (0.3244×10^{-5})	0.9309×10^{-3} (0.1002×10^{-5})	0.8502×10^{-3} (0.9151×10^{-6})
Response error cm^2/sec^2 (ft^2/sec^2)	$0.1083 \times 10^{+1}$ (0.1166×10^{-2})	0.2220×10^{-1} (0.2390×10^{-4})	0.1826×10^{-1} (0.1965×10^{-4})	0.1049×10^{-1} (0.1129×10^{-4})	0.9615×10^{-2} (0.1035×10^{-4})
Condition number	0.5945×10^{4}	0.5143×10^{5}	0.1030×10^{8}	0.3723×10^{8}	0.7895×10^{5}
Determinant	0.7486	0.2854×10^{2}	0.7836×10^{5}	0.2462×10^{9}	0.2519×10^{13}
Determinant ratio DV(m)	0.3812×10^{2}	0.2746×10^{4}	0.3142×10^{4}	0.1023×10^{5}	
$\bar{A}$	1.3098	3.7552	3.7359	4.4570	4.3992
Poles	0.4797±i0.7237	0.6519 0.3973±i0.9088	0.3521 0.6527 0.3965±i0.9088	0.4615 -0.4778 0.8696 0.3951±i0.9061	0.8386 -0.6826 0.3397±i0.2289 0.3940±i0.9060
Zeros		-6.5969	0.3639 -6.7253	-0.8471 0.8358 -6.5044	0.1356 0.7680 -0.9320 -6.5072

Table 1. Results of Model Order Tests for $\dot{x}_p/V_{rv}(z)$

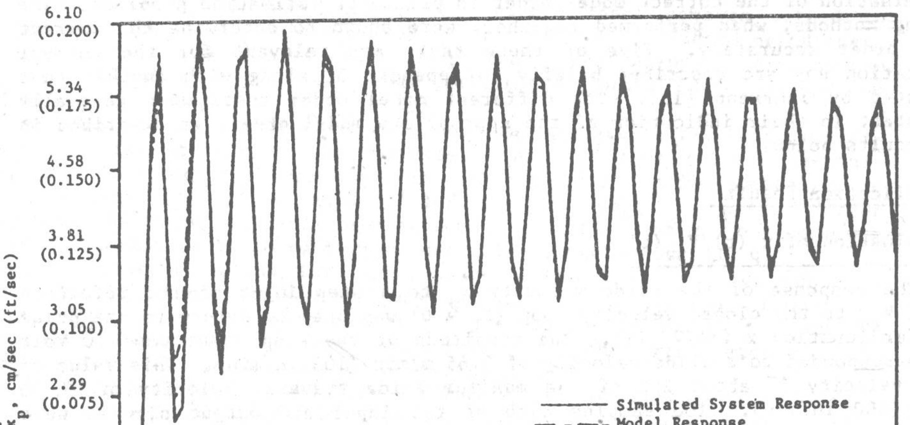

Figure 2. Response of Simulated System and Third Order Least Squares Models to Unit Step Input of V_{rv}

The model order tests, when applied to the results in Table 1, indicate that the appropriate model order is three. An increase in the model order from two to three resulted in the largest reduction in the error measures. The condition number registered a sharp increase for an increase in the model order from three to four. Poor numerical conditioning of the identification problem for model orders of four or higher is also indicated by the determinant ratio test. The polynomial test requires examination of the zeros and poles of the pulse transfer function. For a model order of four, there is a near cancellation of a pole and a zero. The remaining poles and zeros approximate those for the third order model well. Isermann's step response invariance test [18] indicates that the model response changes significantly for a change in the model order from two to three but does not change when the model order is increased to four. The model step response changes somewhat when the model order is increased to five but, in view of the results from the other tests, a model order of three is chosen as the most appropriate one.

Figure 2 shows a plot of the simulated system response and the response of the third order model to a step input of V_{rv} of 1.0 volt. Model parameters are indicated on the figure. The model response is a very good approximation of the simulated system response. In view of the SCR amplifier nonlinearity, the response of this third order model to rectangular and triangular pulse inputs of V_{rv} was determined and compared to the system response. The results are shown by Figures 3 and 4. The rectangular pulse height and duration were 1.0 Volt and 16 milliseconds respectively. The triangular pulse height and duration were 0.5 Volts and 100 milliseconds respectively. Model response to a variety of other inputs was also evaluated and compared with system response.

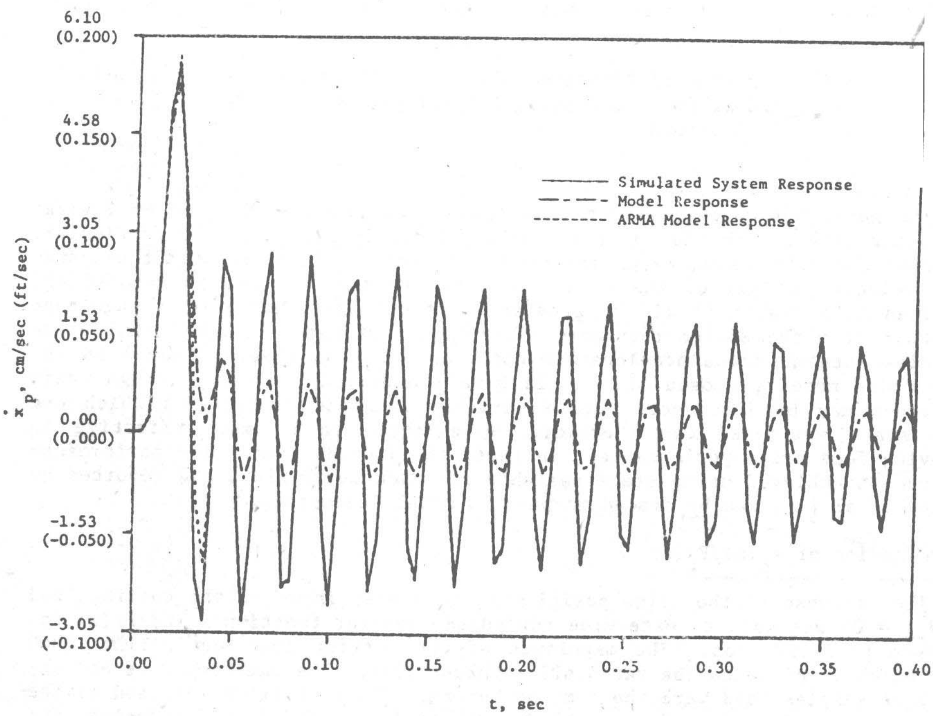

Figure 3. Response of Simulated System and Third Order Least Squares Models to a Rectangular Pulse Input of V_{rv} - Size 1V, Duration 0.016 seconds

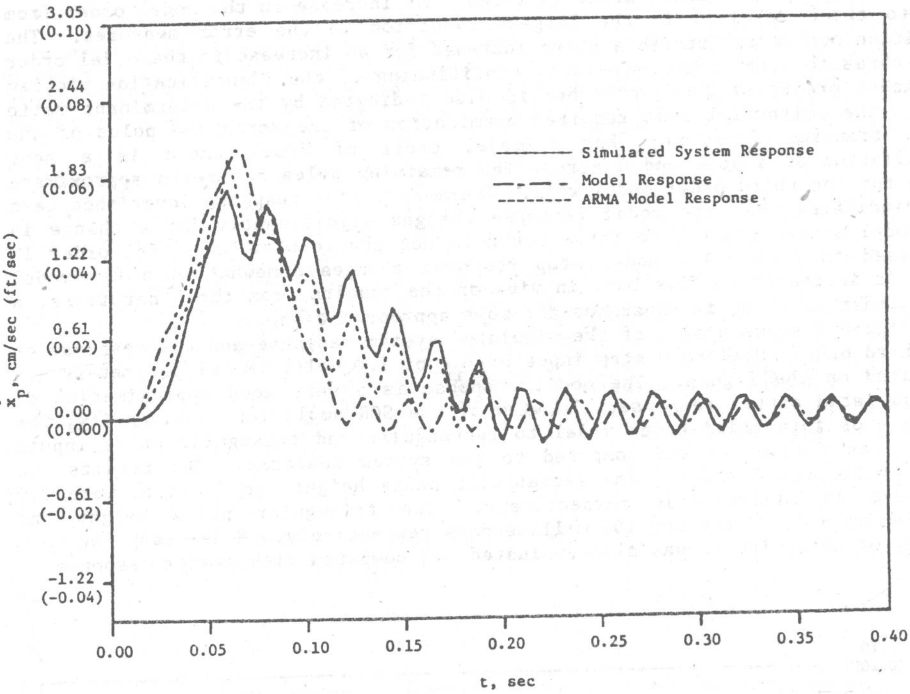

Figure 4. Response of Simulated System and Third Order Least Squares Models to a Triangular Pulse Input of V_{rv} - Peak 0.5V at 0.05 seconds

The model response agreement with the system response denoted by Figures 2-4 is far better than that of any models previously proposed. In particular, note that the slide velocity predicted by the model is in phase with the system slide velocity in all of these figures, whereas the two models proposed and evaluated by Kulkarni et al [7] predicted outputs that differed in magnitude and phase from the system response. Therefore, estimates of additional state variables such as slide acceleration obtained using an observer based on the third order model proposed here would have the correct polarity though their magnitudes may be incorrect. State variable feedback controllers which use these state estimates can therefore be expected to be more effective in improving feed drive performance. In fact, the limited feed drive performance improvement achieved using state variable feedback controllers and reported by Johnson et al [16] can be traced in part to model inaccuracy.

Determination of $x_p(z)/F_L(z)$

The response of the slide position x_p to a step input of the cutting load F_L (V_{rv} = 0) was used to determine the pulse transfer function $x_p(z)/F_L(z)$ for the open position loop. The magnitude of the cutting load was 10230N (2300 lbf), which is close to the rated slide thrust load. The sampling rate and the number of samples used were the same as before. Slide position was used as the output signal instead of the slide velocity in order to increase the significance of low frequency components in the output signal relative to the high frequency components caused by the mechanical transmission resonance. The dominant components in feed drive compliance to cutting loads are at lower frequencies [16]. Hence the need for accuracy in modeling the low frequency components of the feed drive response to cutting loads. The low frequency components can be detected in the slide velocity also but would require much higher model orders.

Pulse transfer function models of the form of equation (2) and of orders two to five were identified for $x_p(z)/F_L(z)$. Table 2 indicates the results of applying the model order tests described in Appendix B. The model tests for $x_p(z)/F_L(z)$ are less conclusive than for $\dot{x}_p(z)/V_{ry}(z)$ but suggest that a model order of four is appropriate. An increase in the model order from three to four results in a tenfold reduction of the equation error. Further increase in

Model Order, m	2	3	4	5
Equation error cm^2 (ft^2)	0.4243×10^{-1} (04567×10^{-4})	0.1623×10^{-1} (0.1747×10^{-4})	0.5014×10^{-2} (0.5397×10^{-5})	0.4021×10^{-2} (0.4328×10^{-5})
Response error cm^2 (ft^2)	0.7360×10^{-1} (0.7922×10^{-4})	0.9467×10^{-1} (0.1019×10^{-3})	0.5445×10^{-1} (0.5861×10^{-4})	0.5771×10^{-1} (0.6212×10^{-4})
Condition number	0.2246×10^{10}	0.1044×10^{11}	0.1627×10^{12}	0.6132×10^{13}
Determinant	0.6370×10^{9}	0.3111×10^{8}	0.1040×10^{24}	0.3713×10^{32}
Determinant ratio DV(m)	0.4884×10^{7}	0.3343×10^{8}	0.3570×10^{9}	
$\tilde{A}$	0.2172×10^{2}	0.2637×10^{2}	0.2087×10^{2}	0.2050×10^{2}
Poles	0.4440 0.9531	0.9631 0.4197±i0.1835	0.7890 0.9420 0.3970±i0.8801	0.7937 -0.5435 0.9393 0.3976±i0.8776
Zeros	0.2781	-0.0487±i0.8512	0.8433±i0.4010 -1.0615	-0.8283±i0.1237 0.8707±i0.4017

Table 2. Results of Model Order Tests for $x_p/F_L(z)$

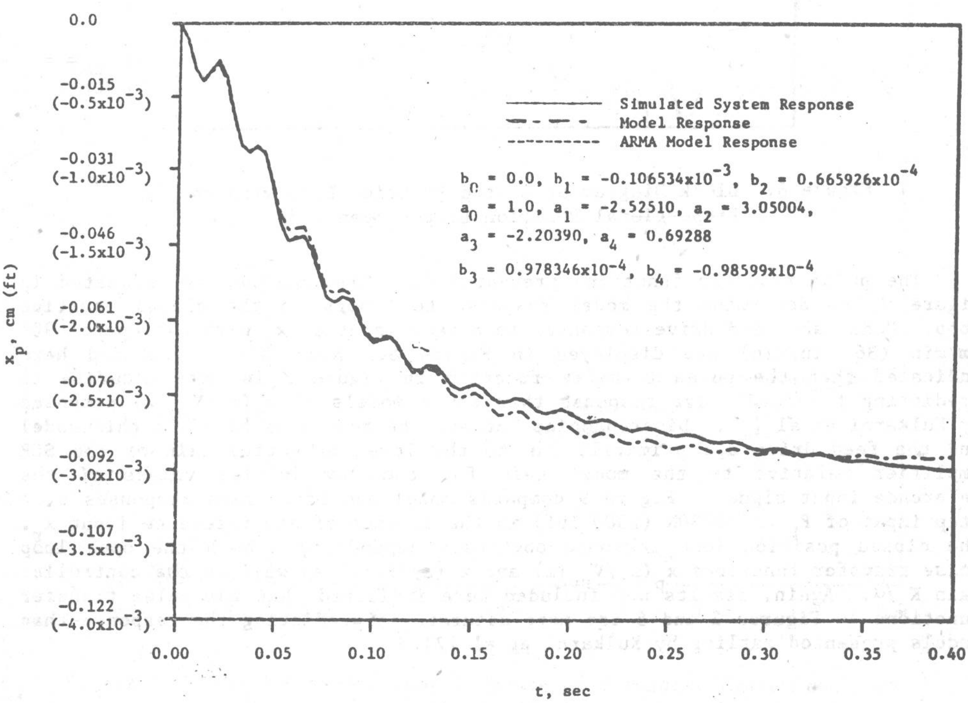

Figure 5. Response of Simulated System and Fourth Order Least Squares Models to a Step Input of F_L - 10230N(2300 lbf)

试读结束：需要全本请在线购买： www.ertongbook.com